Purdue University
Purdue e-Pubs

International Refrigeration and Air Conditioning Conference

School of Mechanical Engineering

2014

Modeling of Lubricant Effects in a Microchannel Type Condenser

Andrea A. M. Bigi
Oklahoma State University, United States of America, abigi@okstate.edu

Lorenzo Cremaschi
Oklahoma State University, United States of America, cremasc@okstate.edu

Daniel E. Fisher
Oklahoma State University, United States of America, dfisher@okstate.edu

Modeling of Lubricant Effects in a Microchannel Type Condenser

Andrea A. M. BIGI[1]*, Lorenzo CREMASCHI[1], Daniel E. FISHER[1]

[1]Oklahoma State University, School of Mechanical and Aerospace Engineering,
Stillwater, OK, USA

* Corresponding Author: Ph. (405)-744-0389, email: abigi@okstate.edu

ABSTRACT

In HVAC and refrigeration systems, a small portion of the oil circulates with the refrigerant flow through the cycle components, while most of the oil stays in the compressor. The circulating oil can form a fairly homogeneous mixture with the liquid refrigerant, or it can exist as a separate oil-rich film inside the small tubes and headers of a microchannel heat exchanger; the amount of oil held up is affected by the system conditions. The oil retention in the microchannel type condenser is of particular interest as the amount of oil in excess in this component affects the heat transfer capacity and increases the frictional pressure losses. This paper presents a new physics-based model of the oil retention in microchannel-type condensers. The model calculates the local thermodynamic properties in each section for the refrigerant R-410A and Polyester (POE) oil mixture based on the local oil concentration, pressure, temperature, and mass flux. Then the model, which was experimentally validated, predicts the refrigerant-side heat transfer coefficient and pressure drop. The simulation results indicated that the pressure losses increased by over 20% when the oil mass flow rate fraction increased up to 5 weight percent. The augmented mixture viscosity resulted in high frictional pressure drops and shear stress during the two phase flow condensation. The refrigerant side correlations were validated against literature data for in-tube two-phase flow condensation but further investigation is needed for the single-phase annular type flow in microchannel with refrigerant vapor and oil. At low degree of superheat the heat transfer coefficient of the refrigerant and oil mixture was basically unaffected by the oil mass fraction up to 3 weight percent. When the oil mass fraction was higher than 3 weight percent, then the heat transfer capacity of the condenser decreased. At high degree of superheat, the heat transfer coefficient of the oil and refrigerant mixture was penalized when the Oil Mass Fraction (OMF) was higher than 2 weight percent. Further investigation is needed on the suitability and accuracy of the heat transfer coefficients correlations to be adopted with superheated vapor refrigerant and lubricant film in annular flow at the inlet section of the microchannel type condenser.

1. INTRODUCTION

In HVAC and refrigeration systems, oil is used because the compressor moving parts need to be lubricated. The refrigerant circulating in the system is mixed with some of the oil inside the compressor and a small amount of oil is carried through the refrigeration system components. In the heat exchangers and pipelines, the lubricant in excess creates small layers on the internal surfaces, which add thermal resistance to the heat transfer exchange process and augment the frictional pressure losses. When oil is present, the heat transfer rate and the pressure drop of the heat exchangers are often penalized. Hence, the efficiency of the system is also reduced. Microchannel type condensers have unique oil retention characteristics because of their small internal volume and of their header configuration. For microchannel heat exchangers, different models were developed to predict the heat transfer coefficient and to optimize the design of the heat exchanger for high performance. Often the models were based on a control volume approach and used an effectiveness-NTU method (Incropera and DeWitt, 1996) to solve the heat balance between the air side and the refrigerant side. Huang et al. (2012) developed a model to investigate various heat exchanger tube geometries. Schwentker et al. (2005) developed a design tool for microchannel heat exchangers. The model developed in this paper used a similar approach and it is based on the heat exchanger model originally developed by Iu (2007). The user defines the coil geometry parameters and selects the appropriate heat transfer and pressure drop correlations. Several researchers investigated correlations to predict the heat transfer and the pressure drop of both the refrigerant side and air side in condensers. For example, Chang et al. focused on louvered fins used for microchannel coils and they developed correlations for heat transfer coefficient (1997) and for friction factors (2000). The behavior of the refrigerant and oil mixture during a condensation processes is also available in the literature (Bassi and Bansal, 2003; Schlager et al., 1990; Thome, 1995). In 2010, Huang et al. investigated the influence of oil on condensation heat transfer coefficient of R-410A for tubes of nominal diameters smaller the 5 mm. Their correlations are used in the present work as it is discussed later. From this brief literature summary it appears that there are several models that are able to predict the heat transfer rate and pressure drop of refrigerant R-410A two-phase flow condensation in microchannel condensers but they do not often consider the presence of oil in circulation with the refrigerant nor they have been experimentally verified when oil is retained in the condenser. This paper presents a new physics-based experimentally validated model of the oil retention in microchannel-type condensers. The model uses a segmentation method to divide the heat exchanger into small sections along the refrigerant flow. By imposing a heat balance and by using the effectiveness-NTU method, the outlet conditions are predicted for each section and passed as input for the adjacent section until the entire refrigerant circuitry is completed. The model calculates the local thermodynamic properties in each section for the refrigerant R-410A and Polyester (POE) oil mixtures based on the local oil concentration, pressure, temperature, and mass flux. Then the model predicts the volume of oil retained in the microchannel tubes and its influence on the refrigerant-side heat transfer coefficient and pressure drop. The microchannel condenser used for model validation was for a 4-ton nominal capacity of a R-410A air conditioning system for residential applications and the microchannel tube hydraulic diameter was about 1.7 mm.

2. MODEL DEVELOPMENT

The condenser coil tested for the present work was a 2 passes microchannel type heat exchanger with horizontal tubes and vertical headers. The condenser section consisted of the top section of the heat exchanger and included the top 69 tubes while the bottom 32 tubes were used for subcooling. With the assumption of uniform refrigerant flow distribution and uniform air velocity and temperature entering the heat exchanger, the model simplified the condenser and the subcooler section to single tubes connected in series, as shown at the bottom in Figure 1. Periodic boundary conditions to the single tubes were applied to the condenser tube and to the subcooler tube to estimate the capacity of the heat exchanger. Each tube had four ports and a single line of fins and the refrigerant flow rate was proportionally scaled. It should be noticed that the refrigerant mass flow rate per port was higher in the subcooler because the subcooler had fewer tubes. A segmentation method is shown at the right side of Figure 1 and each single tube heat exchanger was divided into a large number of small control volume elements. Each control volume was solved iteratively before proceeding to the adjacent control volume. Heat transfer coefficient correlations and pressure drop correlations for single and for two phase flow of refrigerant and oil mixtures were used in each control volume. The air entering velocity was uniform across the entire face area of the heat exchanger and thus the air flow rate was scaled based on the face area of each control volume. After computing the capacity of each control volume, the outlet pressure and enthalpy of the refrigerant were passed to the adjacent control volume as inputs, until the refrigerant circuitry was solved from inlet to outlet of the heat exchanger.

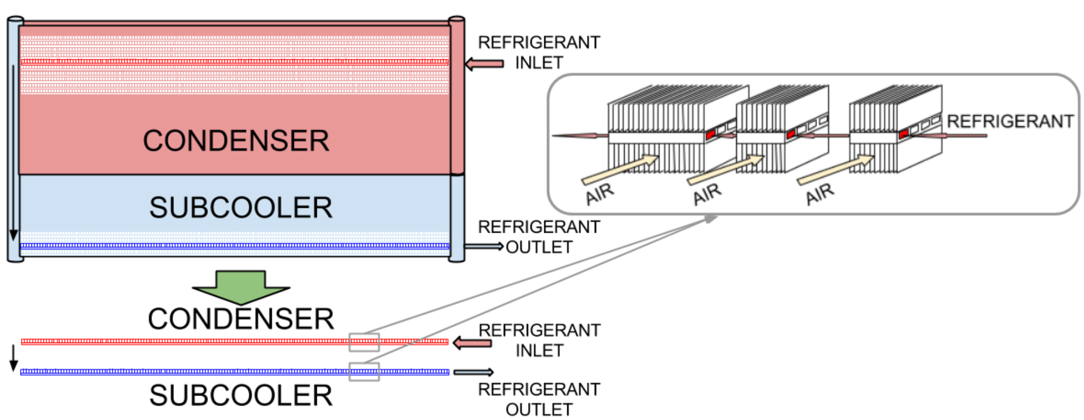

Figure 1: Full scale microchannel heat exchanger (top left), model of the heat exchanger with two tubes (bottom left) and details of the control volume approach for each tube (right)

2.1 Assumptions of the model

The main assumptions and simplifications of the present model were as follows:

- The coil headers were neglected both in the calculations of the heat transfer rate and pressure drops
- Uniform refrigerant distribution and uniform air velocity and air temperature entering the heat exchanger
- The amount of oil trapped in the headers was also neglected
- The air dry bulb temperature and relative humidity at the outlet of the microchannel coil were calculated from a weighted average based on the number of tubes present in the condenser part and in the subcooler part of the coil

2.2 Air Side Correlations

The air flow at the inlet of the microchannel heat exchanger was characterized by three inlet parameters: the air flow rate, the dry bulb temperature and the relative humidity. The calculation of the j-factor for the air heat transfer coefficient was based on the correlations by Chang and Wang (1997) shown in Equation (1).

$$\mathrm{j} = \mathrm{Re}_{\mathrm{Lp}}^{-0.49}\left(\frac{\theta}{90}\right)^{0.27}\left(\frac{\mathrm{F_p}}{\mathrm{L_p}}\right)^{-0.14}\left(\frac{\mathrm{F_l}}{\mathrm{L_p}}\right)^{-0.29}\left(\frac{\mathrm{T_d}}{\mathrm{L_p}}\right)^{-0.23}\left(\frac{\mathrm{L_l}}{\mathrm{L_p}}\right)^{0.68}\left(\frac{\mathrm{T_p}}{\mathrm{L_p}}\right)^{-0.28}\left(\frac{\delta_\mathrm{f}}{\mathrm{L_p}}\right)^{-0.05} \quad 100 < Re_{\mathrm{Lp}} < 3000 \tag{1}$$

This correlation is valid for corrugated fin geometry and in the comparison with experimental data, it gives a mean deviation of about 8%. The friction factor for the air pressure drop calculation is based on the friction correlations for louver fins by Chang *et al.* (2000) that is summarized in Equation (2).

$$\mathrm{f} = \mathrm{f_1} * \mathrm{f_2} * \mathrm{f_3} \tag{2}$$

Where f_1, f_2, f_3 are functions of geometry parameters and are summarized in Equations (3), (4) and (5):

$$\mathrm{f_1} = \begin{cases} 14.39\,\mathrm{Re}_{\mathrm{Lp}}^{(-0.805\mathrm{F_p}/\mathrm{F_l})}\left(\log_e(1.0 + (\mathrm{F_p}/\mathrm{L_p}))\right)^{3.04} & \mathrm{Re_{Lp}} < 150 \\ 4.97\mathrm{Re}_{\mathrm{Lp}}^{0.6049-1.064/\theta^{0.2}}\left(\log_e((\mathrm{F_t}/\mathrm{F_p})^{0.5} + 0.9)\right)^{-0.527} & 150 < Re_{\mathrm{Lp}} < 5000 \end{cases} \tag{3}$$

$$\mathrm{f_2} = \begin{cases} \left(\log_e\left((\mathrm{F_t}/\mathrm{F_p})^{0.48} + 0.9\right)\right)^{-1.435}\left(\mathrm{D_h}/\mathrm{L_p}\right)^{-3.01}\left(\log_e(0.5\mathrm{Re_{Lp}})\right)^{-3.01} & \mathrm{Re_{Lp}} < 150 \\ \left((\mathrm{D_h}/\mathrm{L_p})\log_e(0.3\mathrm{Re_{Lp}})\right)^{-2.966}\left(\mathrm{F_p}/\mathrm{L_l}\right)^{-0.7931(\mathrm{T_p}/\mathrm{T_h})} & 150 < Re_{\mathrm{Lp}} < 5000 \end{cases} \tag{4}$$

$$\mathrm{f_3} = \begin{cases} \left(\mathrm{F_p}/\mathrm{L_l}\right)^{-0.308}(\mathrm{F_d}/\mathrm{L_l})^{-0.308}\left(e^{-0.1167\mathrm{T_p}/\mathrm{D_m}}\right)\theta^{0.35} & \mathrm{Re_{Lp}} < 150 \\ \left(\mathrm{T_p}/\mathrm{D_m}\right)^{-0.0446}\log_e\left(1.2 + (\mathrm{L_p}/\mathrm{F_p})^{1.4}\right)^{-3.553}\theta^{-0.477} & 150 < Re_{\mathrm{Lp}} < 5000 \end{cases} \tag{5}$$

The comparison with experimental data of the literature, this correlation had a mean deviation of about 9 to 10%.

2.3 Refrigerant Side Correlations

The inlet conditions of the refrigerant were defined by four parameters: the oil absolute mass fraction, the mass flow rate, the enthalpy and the pressure. Shen and Groll (2003) observed that the lubricant vapor pressure is negligible when compared to the refrigerant vapor pressure and therefore the presence of oil does not affect the mixture vapor pressure. The heat transfer coefficient and the pressure drop were calculated as a function of the refrigerant quality. When lubricant is present in the simulation, refrigerant properties are corrected as a function of the local oil mass fraction (Cremaschi, 2005). In the single phase region the refrigerant heat transfer coefficient was calculated using Gnielinski correlation (1976). However, when oil is present, the mixture quality (x_{mix}) is defined as in Equation (6).

$$\mathrm{x_{mix}} = \dot{\mathrm{m}}_{\mathrm{ref,gas}}/(\dot{\mathrm{m}}_{\mathrm{ref,gas}} + \dot{\mathrm{m}}_{\mathrm{ref,liq}} + \dot{\mathrm{m}}_{\mathrm{oil}}) \tag{6}$$

Where $\dot{m}_{ref,gas}$ and $\dot{m}_{ref,liq}$ are the refrigerant vapor and liquid mass flow rates and $\dot{m}_{oil}$ is the oil mass flow rate. Since oil never enters the vapor phase, the mixture quality is always lower than one, even when the refrigerant is in the superheated region. For this reason, when oil is present, the mixture is always in a two-phase flow until the refrigerant condensation is completed. In order to account for the presence of oil in the calculation of the condensation heat transfer, Huang *et al.* (2010) proposed a correlation describing the condensation characteristics of R-410A and oil mixture for horizontal smooth tubes with inner diameter of 4.18 and 1.6 mm and for a range of nominal oil concentration varying from 0 to 5%. In the correlation suggested (see Equation (7)), the condensation Nusselt number is calculated taking account of both a forced convection expressed by Equation (8) and a free convection component expressed by Equation (9).

$$\mathrm{Nu} = \alpha_{tp,r,o} D_h/\lambda_L = \left(\mathrm{Nu}_F^2 + \mathrm{Nu}_B^2\right)^{0.5} \tag{7}$$

$$\mathrm{Nu}_F = 0.0152(\Phi_V/X_{tt})\mathrm{Re}_L^{0.77}(a + b\mathrm{Pr}_L^{0.8}) \tag{8}$$

$$\mathrm{Nu}_B = 0.725H(\varepsilon)(\mathrm{Ga}_L\mathrm{Pr}_L/\mathrm{Ja}_L)^{0.25} \tag{9}$$

Where Φ_V is a two phase frictional multiplier, $H(\varepsilon)$ is a function of the void fraction and a and b are coefficients determined by linear regression to fit the experimental data, as reported in Huang *et al.*(2010). The calculation of the refrigerant pressure drop is also dependent on the refrigerant quality. The pressure change in the single phase region was computed using Fanning friction factor as described in Ragazzi and Pederson (1999). For the two phase area, the semi-empirical approach proposed by Lockhard-Martinelli (1949) was applied as described in Cremaschi (2005).

2.4 Model Implementation and Converging Criteria

The present work used a heat exchanger numerical solver that was developed by Iu (2007) for a heat pump system. The model was implemented in FORTRAN and each single tube was divided in multiple segments whose capacity was computed using an effectiveness-NTU method. The air inlet conditions were constant for each segment while the refrigerant conditions at the inlet of each segment were obtained from the outlet conditions calculated for the previous adjacent segment. The correlation for the calculations of the refrigerant heat transfer coefficient required the computation of the Jacob number (Ja) as shown in Equation (9). The Jacob number is the ratio of sensible to latent heat absorbed during the process of liquid-vapor phase change and it is described in Equation (10):

$$\mathrm{Ja} = C_p\left(T_{s,guessed} - T_{sat}\right)/\Delta H_f \tag{10}$$

Where ΔH_f is the latent heat of condensation, C_p is the fluid heat capacity and $T_{s,guessed}$ and T_{sat} are respectively the surface temperature of the tube wall and the fluid saturation temperature. The wall surface temperature was not known a priori and therefore, an iterative process was used to calculate the Jacob number. From a first guess value the refrigerant heat transfer coefficient was estimated, the segment capacity was calculated using the effectiveness-NTU method for cross-flow heat exchangers. The new value of the wall surface temperature was then computed from the energy balance on the elemental control volume (that is, on each segment of the coil along the refrigerant direction) as shown in Equation (11):

$$T_{s,computed} = T_{air,inlet} + Q_{seg} * R_{air} \tag{11}$$

Where $T_{air,inlet}$is the air inlet temperature, $Q_{seg}$is the segment capacity and $R_{air}$is the air side heat transfer total resistance calculated using the j-factor correlation of Equation (1). The flow chart of the model implementation in the heat exchanger simulator is shown in Figure 2. The initial guess values of surface temperature was corrected until the difference with the guessed value between two consecutive iteration was less than 0.1ºC. Segment by segment along the forward direction of the refrigerant flow, the procedure shown in Figure 2 was repeated for the entire heat exchanger. In addition, a spreadsheet interface was developed as a tool to analyze the simulation data and compare the prediction from the simulation with experimental data when available. The spreadsheet, which was developed using Visual Basic and Excel, reproduces a schematic of the microchannel condenser coil and allows to compare simulation results with experimental data and to calculate the simulation error of the outlet conditions for both the air and the refrigerant side. The coil was mainly divided into five large sections along the direction of the refrigerant flow in order to better observe the trends of temperature and pressure from the simulation results and the corresponding experimental data.

3. EXPERIMENTAL DATA FOR MODEL VALIDATION

Experimental data of the effect of oil on the heat transfer rate and pressure drop of microchannel type condensers were measured and were used to validate the predictions from the present model. The microchannel condenser used for model validation was for a 4-ton nominal capacity of a R410A air condition system for residential applications and the microchannel tube hydraulic diameter was about 1.7 mm. and the geometry of the microchannel heat exchanger is given in Table 1. The microchannel type condenser coil was tested at different operation conditions with refrigerant R-410A only first and then with refrigerant R-410A and POE lubricant. The experimental data were obtained for two level of degree of superheat entering the condenser: one with low degree of superheat and one with high degree of superheat. The experimental setup, the test procedures, and test conditions for the experimental data of the microchannel condenser were described in details in a companion paper (Yatim *et al.* 2014). For completeness they are briefly summarized next. The heat exchanger was tested at different operational conditions both with refrigerant R410A and with a refrigerant-POE oil mixture; the saturation temperature ranged from 29 to 54 °C and the refrigerant flow rate was varied between 0.05 and 0.08 kg/s. Finally, the oil mass fraction was also varied from 0.5 to 5% in order to observe the rate of refrigerant heat transfer decay and pressure drop increase.

Table 1: geometry parameters

Parameter	**Value**
Coil Height [mm]	908
Coil Depth [mm]	1215
Fin type	Louvered
Channel nominal inside diameter [mm]	1.7
Number of channels per tube	4
Number of pass	2
Number of condenser tubes	69
Number of subcooler tubes	32

The microchannel was assembled inside a psychrometric chamber that allows for control of the air dry bulb temperature and relative humidity. Air was moved by a fan installed after the heat exchanger coil and air mass flow rate was measured by pressure difference across air nozzles. A grid of twenty thermocouples was installed at a distance of about 3 centimeters after the microchannel coil allowing for temperature measurement at the outlet of the heat exchanger. On the refrigerant side, temperature and pressure sensors were installed at the inlet and outlet of the coil header; refrigerant mass flow rate was measured using a mass flow meter installed before the coil. Using a variable frequency drive-controlled oil gear pump, the oil flow rate was controlled and oil was injected both at the inlet and at the outlet of the heat exchanger. In order to calculate the oil retention in the microchannel heat exchanger, the parameters observed were the flow rate of the injected oil and the timing required by the oil to reach the outlet of the oil separators. By integrating the oil flow rate over time, the amount of oil retained in the microchannel was then estimated by computing the difference between the amount of oil injected at the inlet and that injected at the outlet of the section. The air heat transfer capacity and the refrigerant pressure drop were monitored while injecting the oil and then compared with the same values observed when running the system at the same operational conditions but with no oil. The accuracy of the instrumentation is reported in Table 2. Moreover, thermal images of the front of the coil were recorded in order to measure the coil surface temperature and check for the uniformity of the refrigerant flow distribution in the condenser.

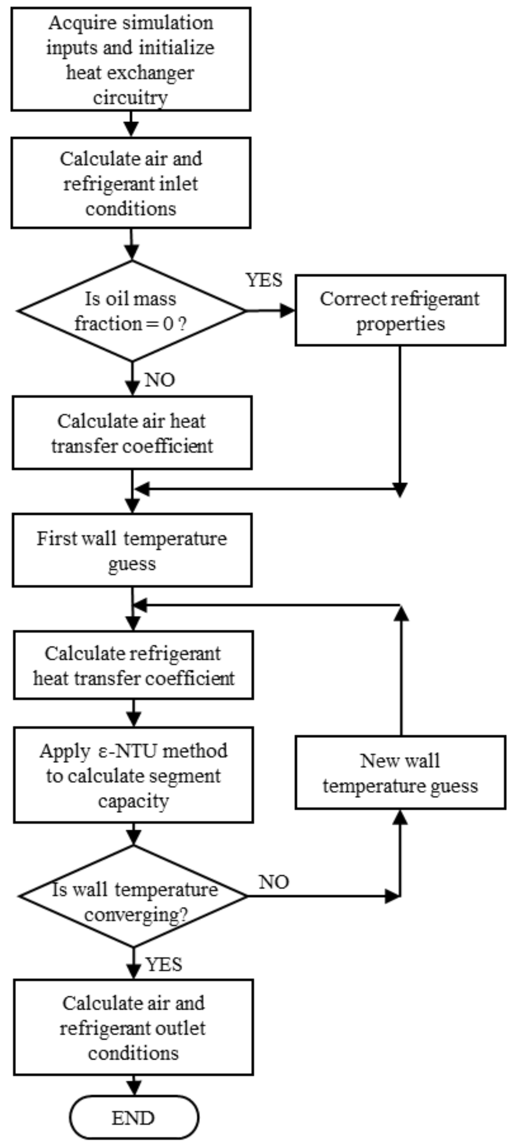

Figure 2: Flow chart of the model implementation in the numerical FORTRAN solver

Table 2: Experimental uncertainties in the data used for validation of the present model

Parameter	Symbol	uncertainty
Pressure	P	±0.7 psi
Pressure difference	ΔP	±0.03 psi
Temperature	T	±0.1 °F
Mass flow rate	$\dot{m}$	±0.1 %
Air volume flow rate	CFM	±0.4 %

Parameter	Symbol	uncertainty
Oil mass fraction	OMF	0.5 %
Oil retention volume	ORV	1 %
Pressure drop factor	PDF	2 %
Heat transfer factor	HTF	3 %

4. MODEL VALIDATION

Before validating the model with the data of the present work, the air side heat transfer and the refrigerant side heat transfer and pressure drop with and without oil were independently verified with data from the literature. This was done to decouple the air side from the refrigerant side and isolate any potential sources of error in the model implementation. The numerical solver and algorithm was validated by Iu (2007). The air side heat transfer coefficients were verified with the correlations provided by Moallem *et al*. (2013), which were valid for a broad range louvered fin geometries commonly adopted in microchannel condensers. The fin width, fin height, and fin depth of the present work were in the range of the correlation provided in Moallem *et al*. (2013).

4.1 Validation of the refrigerant side heat transfer coefficient with data from the literature

The predictions of the refrigerant two phase flow condensation heat transfer coefficient for oil-R410A mixture at different oil concentrations were verified against the literature data presented in Huang *et al.* (2010) and the results are reported in Figure 3. Figure 3 shows the simulation results of the present model for the heat transfer coefficient at different oil concentrations. The heat transfer coefficient was predicted with an error between ±30% and the model underpredicted the data of heat transfer coefficient. The deviation were larger at low oil concentration. In agreement with the data by Huang *et al.* (2010), the two phase flow condensation heat transfer coefficient was lower for higher oil concentrations. However, the prediction from the present model did not show a decrease of refrigerant side heat transfer coefficient as that reported by Huang *et al* (2010).

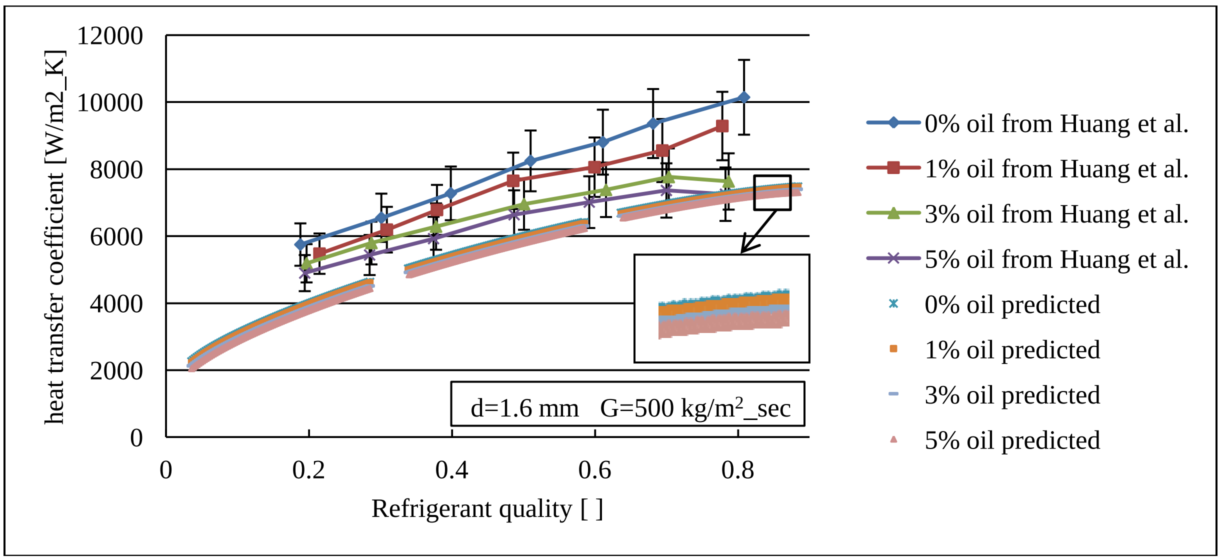

Figure 3: Verification of the refrigerant side heat transfer coefficient with literature data (Huang *et al.* (2010))

4.2 Validation of the heat transfer coefficients and pressure drops with data from the present work

The local surface temperature of the microchannel tube was predicted by the model and it was compared with the data gathered by using a thermal camera. The thermal measurements were taken by using an infrared camera (Fluke Infrared Solutions IR FlexCam), which had an accuracy of ±1°C (~±2°F) and a surface thermocouple (T-type thermocouple) was used for calibrating the emissivity in the images taken with the infrared camera. Figure 4a shows the thermal image of the microchannel condenser for one test and the center tube within the rectangular box was selected as representative tube for the condenser section average surface temperature along the refrigerant flow. Figure 4b shows the comparison of the tube surface temperature between the data and the simulation results. The case reported in here is for a high degree of vapor superheat of about 36°C (65°F), for which the model had to predict a rapid decrease of surface temperature along the tube near the inlet header. There was some deviation at the inlet region of the microchannel tube when the degree of superheat was high. At the inlet section, the surface temperature predicted by the model was up to 10°C lower than the corresponding data of local surface temperature. In the two phase region, the predicted surface temperature by the model was within ±1°C (~±2°F) with respect to the measured surface temperature. Because the two phase region was the main section contributing to the heat transfer rate of the condenser, even though the error in the superheated region surface temperature was large, the overall error in the predicted cooling capacity was small.

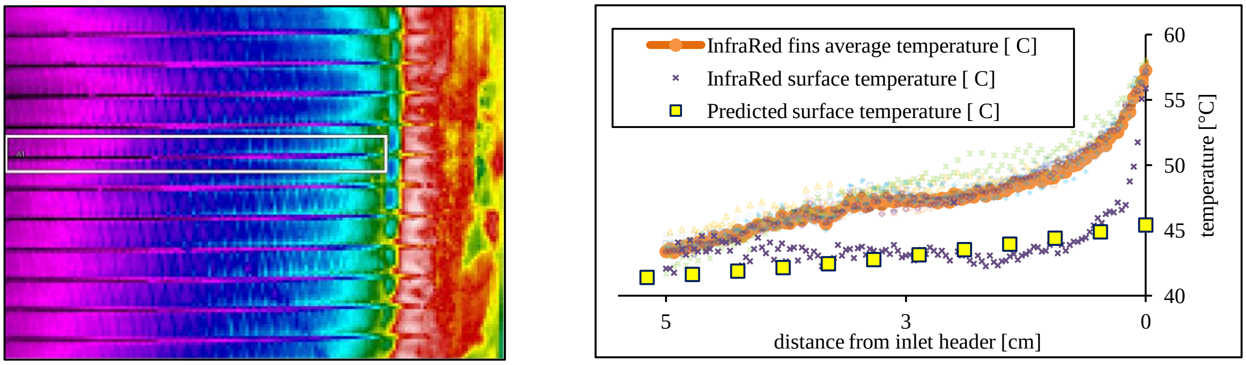

(a) (b)

Figure 4: Infrared image of the MCHX inlet (a) and surface temperature data vs simulation results (b)

After both the air and the refrigerant side heat transfer coefficient and pressure drop were independently verified with data from the literature, the model was further validated with the data and geometry of the present work. The comparisons between experimental and simulation results for the oil free cases are reported in Figure 5. The simulation results of the microchannel type condenser showed a deviation within ±20% with respect to the experimental data and, in general, the simulation prediction tended to overestimate the capacity. The simulation results for the pressure drops had a high discrepancy with respect to the data but it should be noticed that the pressure losses in the headers and in the connecting pipes from the pressure taps to the inlet and outlet ports of the condenser were not accounted for in the simulation model. It is evident that the error in the pressure drop prediction is too large and further investigation is required to address this discrepancy. In particular, more recent works by Sun and Mishima (2009) and Xu and Fang (2013) provide additional correlations for two-phase pressure drop calculation in mini and micro-channels that could be implemented in the present model for improving its accuracy.

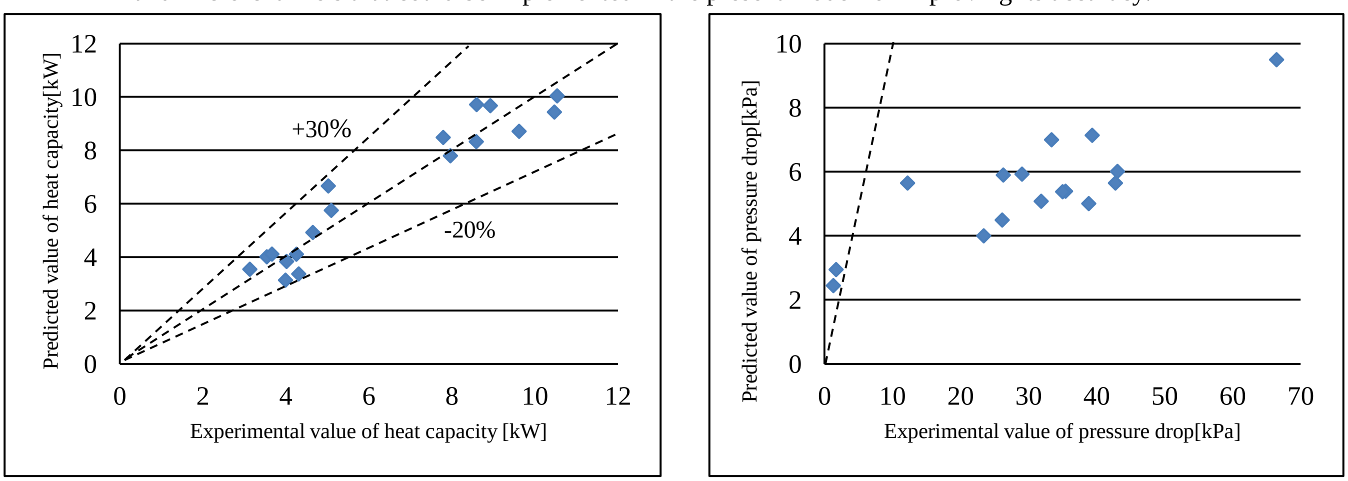

(a) (b)

Figure 5: Comparison between experimental data and predicted results for heat capacity (a) and pressure drop (b)

5. SIMULATION RESULTS AND DISCUSSION

The results are presented for the cases when the refrigerant enters the microchannel heat exchanger at a low degree of superheat and at a high degree of superheat. Simulations were conducted at different oil mass fractions and the predicted heat transfer rate and pressure drop were verified against the experimental data with oil. It should be noticed that the air side velocity and entering temperatures were constant between the case of oil and the corresponding case without oil. Also since the baseline performance with no oil and the performance with oil shared same total mixture flow rate, i.e. the refrigerant flow rate only for the baseline performance and refrigerant plus oil flow rates for the performance with oil were equal, shared same saturation pressure, shared same inlet refrigerant temperature, and shared same air side operating conditions, the results from the comparison between oil and no oil predicted performance provided heat transfer factor and pressure drop factor due to the additional presence of oil in circulation with the refrigerant in the condenser. The oil content of the refrigerant-oil mixture is referred to as the Oil Mass Flow Rate Fraction (OMF) and was calculated as follows:

$$\mathrm{OMF} = \dot{m}_{oil}/(\dot{m}_{ref} + \dot{m}_{oil}) \times 100\% \quad (12)$$

Where $\dot{m}_{oil}$ and $\dot{m}_{ref}$ are respectively the oil and the refrigerant mass flow rates. The Pressure Drop Factor (PDF) and the Heat Transfer Factor (HTF) were computed as shown in Equations (13) and (14), in agreement to the procedure adopted for the experimental data (Yatim *et al*. 2014).

$$\mathrm{PDF} = \Delta P_{@OMF}/\Delta P_{@\,OMF=0} \quad (13)$$

$$\mathrm{HTF} = \dot{Q}_{@OMF}/\dot{Q}_{@OMF=0} \quad (14)$$

Where $\Delta P_{@OMF}$ and $\dot{Q}_{@OMF}$are respectively pressure drop and heat capacity at various oil mass fractions.
The simulation results for the PDF are reported in Figure 6 and the corresponding HTF are reported in Figure 7. The results are reported for saturation temperature of 40.5°C (105°F) and for oil mass fraction from 0 to 5 weight percent and for two refrigerant flow rate representative of full and part load conditions for a 4 ton air conditioning system for residential applications.

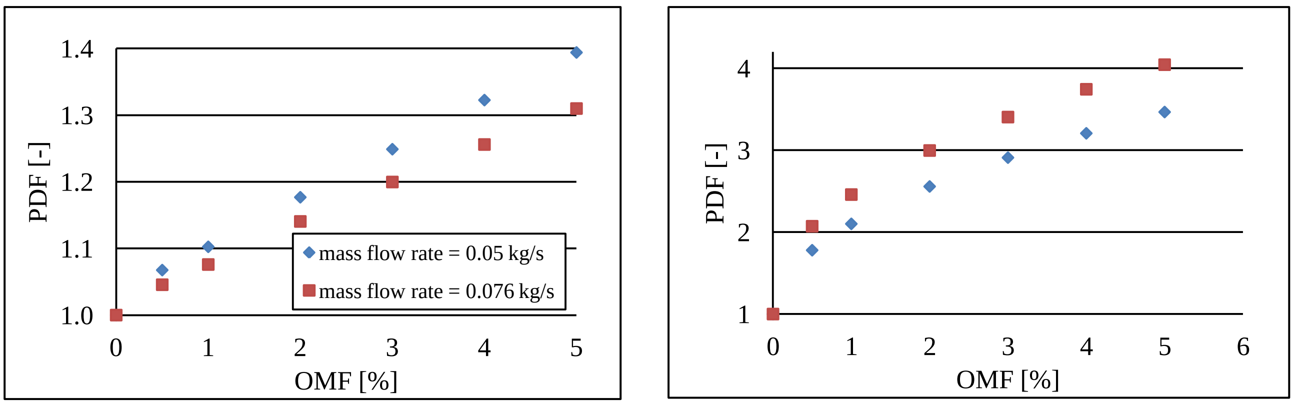

(a) (b)

Figure 6: Pressure Drop Factor (PDF) for (a) low and (b) high degree of superheat

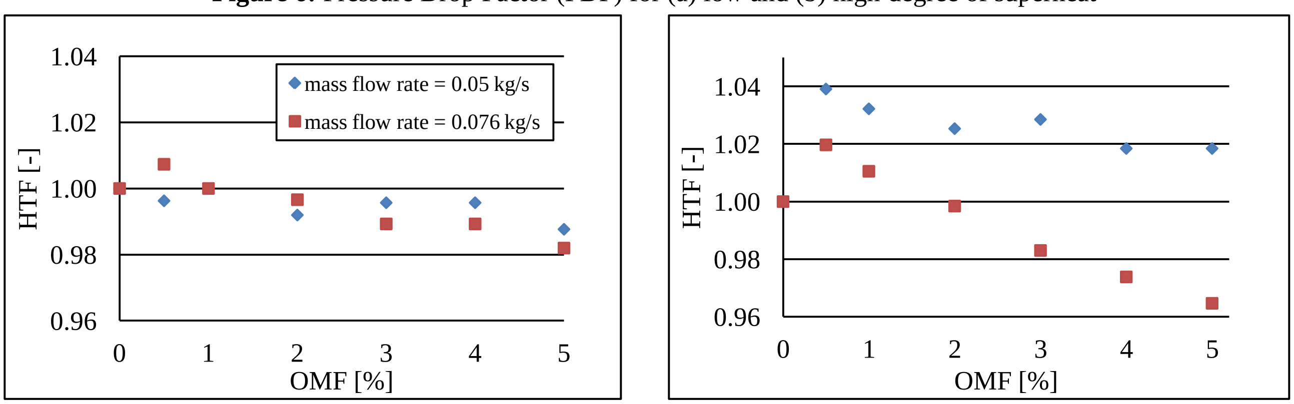

(a) (b)

Figure 7: Heat Transfer Factor for (a) low and (b) high degree of superheat

In Figure 6 the PDF increases if the OMF increases. The magnitude of the simulation results of PDFs for the low degree of superheat (see Figure 6a) was similar to those observed in the experimental data. The increased mixture viscosity resulted in higher frictional pressure drops and shear stress during the two phase flow condensation. At high degree of superheat the simulated PDF were higher. This result was also in agreement with the experimental observations but the magnitude was quite different. The PDF from the experiments increased up to 1.2 while the simulation results showed a PDF of up to 4. This discrepancy might be due to the superheated section of the condenser, in which the oil was present in the inlet header and in the entry region of the tube as excess film layer. The approach proposed by Lockhard-Martinelli (1949) seems not to capture this phenomenon and possible reasons are the different geometry or the nature of the fluid. The HTF tended to decrease if the OMF increased as shown in Figure 7. The data for the low superheat case were in agreement with the experimental data. The HTF was basically unaffected by the OMF up to 3 weight percent and this results was observed in the experimental campaign (Yatim *et al.*, 2014). When the OMF was higher than 3%, the heat transfer capacity of the condenser decreased. At high degree of superheat the HTF predicted by the model showed an unexpected increase of heat transfer at low OMFs. Then the HTC decreased if the OMF was higher than 2%. Similar trends were observed in the experimental campaign reported in a companion paper (Yatim *et al.* 2014). At low mass flow rate, the HTF in Figure 7b was higher than the conditions with no oil present in the condenser. This aspect must be further investigated before drawing general conclusions. In particular the discrepancy of the PDF in Figure 6b might be also responsible for the simulation results in Figure 7b.

6. CONCLUSIONS

This paper presents a new physics-based model of the lubricant effects on heat transfer rates and pressure drops in microchannel-type condensers. The approach of the present model was to divide the heat exchanger coil into a large number of sub-segments along the refrigerant flow and to estimate the local thermodynamic properties of the refrigerant R-410A and POE oil mixture in each sub-segment based on the local oil concentration, local pressure, local temperature, and mass flux inside the microchannel tubes. The present model was experimentally validated against data from the literature and data from a companion paper submitted to this conference (Yatim *et al.* (2014)). The simulation results showed a deviation of about ±20% with respect to the experimental data of heat transfer rate and, in general, the simulation predictions overestimated the data. When lubricant was present in the microchannel type condenser, the heat transfer capacity tended to decrease if the OMF increased. Up to 3 weight percent OMF, the presence of oil did not affect the heat transfer capacity significantly with respect to the oil free case. This result was in agreement with the experimental results reported by the companion paper to this conference for low degree of superheated vapor entering the condenser. When the OMF was higher than 3 weight percent, then the heat transfer capacity of the condenser decreased by up to 4%. At high degree of superheat and for higher mass flow rates, the heat transfer coefficient of the refrigerant and oil mixture was reduced when the OMF was higher than 2 weight percent. The simulation results also predicted an increase in pressure losses by over 20% when the oil mass fraction increased to 5 weight percent. The lubricant in circulation with the refrigerant increased the liquid phase viscosity and therefore the frictional pressure drops and the shear stresses inside the microchannel tubes. Future work include the study of the refrigerant vapor and oil mixtures flow regime in microchannels, the implementation of the additional correlations for heat transfer coefficient and frictional pressure drops for various mixture flow regimes, and the estimation of the pressure losses in the headers, in order to improve the accuracy of the present microchannel condenser model.

NOMENCLATURE

a, b	:	coefficients in Eq. (8)	(-)
D_h	:	hydraulic diameter	(m)
D_m	:	major tube diameter	(m)
f	:	Fanning friction factor	(-)
F_d	:	fin depth	(mm)
F_l	:	fin length	(mm)
F_p	:	fin pitch	(mm)
F_t	:	fin thickness	(mm)
Ga	:	Galileo number	(-)
j	:	Colburn factor	(-)
Ja	:	Jacob number	(-)
L_l	:	louver length	(mm)
L_p	:	louver pitch	(mm)
NTU	:	Number of Transfer Units	(-)
Nu	:	Nusselt number	(-)
Pr	:	Prandtl number	(-)

T_p	:	tube pitch	(mm)
T_h	:	T_p - D_m	(mm)
X_{tt}	:	Martinelli parameter	(-)

Greek symbols

α	:	heat transfer coefficient	(W m^{-2} K^{-1})
δ	:	thickness	(mm)
λ	:	thermal conductivity	(W m^{-1} K^{-1})
θ	:	louver angle	(deg)

Subscripts

B	:	free convection condensation
f	:	fin
F	:	forced convection condensation
L	:	liquid
o	:	oil

Re_{Lp}	:	Reynolds number based on louver pitch	(-)	r	:	refrigerant
				tp	:	two-phase
T_d	:	tube depth	(mm)			

REFERENCES

Bassi, R., Bansal, P. K., 2003, In-tube condensation of mixture of R134a and ester oil: empirical correlation, *International Journal of Refrigeration*, 26(4): p. 402-409.

Chang, Y. J., Hsu, K. C., Lin, Y. T., Wang, C. C., 2000, A generalized friction correlation for louver fin geometry, *International Journal of Heat and Mass Transfer*, 43(12): p. 2237-2243.

Chang, Y. J., Wang, C. C., 1997, A generalized heat transfer correlation for Iouver fin geometry, *International Journal of Heat and Mass Transfer*, 40(3): p. 533-544.

Cremaschi, L., Hwang, Y., Radermacher, R., 2005, Experimental investigation of oil retention in air conditioning systems, *International Journal of Refrigeration* 28(7): p. 1018-1028.

Gnielinski, V., 1976, New equations for heat and mass-transfer in turbulent pipe and channel flow, *International Chemical Engineering*, 16(2): p. 359-368.

Huang, L., Aute, V., Radermacher, R., 2012, A generalized effectiveness-ntu based variable geometry microchannel heat exchanger model, *Proceedings of the 14th International Refrigeration and Air Conditioning Conference at Purdue,* West Lafayette, IN, July 16-19, Paper No. 2191.

Huang, X., Ding, G., Hu, H., Zhu, Y., Peng, H., Gao, Y., Deng, B., 2010, Influence of oil on flow condensation heat transfer of R410A inside 4.18 mm and 1.6 mm inner diameter horizontal smooth tubes, *International Journal of Refrigeration*, 33(1): p. 158-169.

Incropera, F. P., Dewitt, D. P., 1996, *Introduction to Heat Transfer*, 3rd ed. John Wiley & Sons, Inc., New York, NY, p. 410-425.

Iu, I. S., 2007, Development of air-to-air heat pump simulation program with advanced heat exchanger circuitry algorithm, *Doctoral dissertation*, Oklahoma State University.

Lockhart, R., 1949, Proposed correlation of data for isothermal two-phase, two-component flow in pipes, *Chem. Eng. Prog*. 45(1): p. 39-48.

Moallem, E., Cremaschi, L., Fisher, D. E., 2013, Experimental Investigation of Adverse Effect of Frost Formation on Microchannel Evaporators. Part 1: Effect of Fin Geometry and Environmental Effects, *International Journal of Refrigeration*, 36 (6): p. 1762-1775.

Ragazzi, F., 1991, Modular-based computer simulation of an air-cooled condenser, *Air Conditioning and Refrigeration Center,* College of Engineering. University of Illinois at Urbana-Champaign.

Schlager, L., Pate, M. B., Bergles, A. E., 1988, Evaporation and condensation of refrigerant-oil mixtures in a smooth tube and a micro-fin tube, *ASHRAE transactions*, 94(3112): p. 149-166.

Schwentker, R. A., Aute, V., Radermacher, R., Mercer, K., 2005, Simulation and design tool for microchannel heat exchangers, *5th International Conference on Enhanced, Compact, and Ultra-Compact Heat Exchangers: Science, Engineering, and Technology*, Whistler, British Columbia, Canada, September 11-16.

Shen, B., Groll, A., 2003, Critical literature review of lubricant influence on refrigerant heat transfer and pressure drop, *Air-Conditioning and Refrigeration Technology Institute*, Final Report -21CR/611-20080.

Sun, L., Mishima, K., 2009, Evaluation analysis of prediction methods for two-phase flow pressure drop in mini-channels, *International Journal of Multiphase Flow,* 35(1): p. 47-54.

Thome, J. R., 1995, Comprehensive thermodynamic approach to modeling refrigerant-lubricating oil mixtures, *HVAC&R Research*, 1(2): p. 110-125.

Xu, Y., Fang, X., 2013, A new correlation of two-phase frictional pressure drop for condensing flow in pipes, *Nuclear Engineering and Design*, 263(0): p. 87-96.

Yatim, A. S., Cremaschi L., Fisher D. E., 2014, Experimental Measurements of Oil Retention in a Microchannel Condenser for AC Systems, *Proceedings of the 15th International Refrigeration and Air Conditioning Conference at Purdue*, West Lafayette, IN, July 14-17, Paper No. 2325.

ACKNOWLEDGEMENT

The authors gratefully acknowledge funding and support from American Society of Heating, Refrigerating, and Air Conditioning Engineering (ASHRAE) and the technical assistance from the Project Monitor Subcommittee Members and ASHRAE Technical Committee TC 8.4 Air-to-refrigerant Heat Transfer Equipment.